10.24425/acs.2023.145111

*Archives of Control Sciences*
*Volume* 33(LIX), 2023
*No.* 1, *pages 5–23*

# Robot grasping and regrasping kinematics using Lie algebra, the geodesic, and Riemann curvature tensor

Haydar SAHIN

Differential geometry is a strong and highly effective mathematical subject for robot gripper design when grasping within the predetermined trajectories of path planning. This study in grasping focuses on differential geometry analysis utilizing the Lie algebra, geodesic, and Riemann Curvature Tensors (RCT). The novelty of this article for 2RR robot mechanisms lies in the approach of the body coordinate with the geodesic and RCT. The importance of this research is significant especially in grasping and regrasping objects with varied shapes. In this article, the types of workspaces are clarified and classified for grasping and regrasping kinematics.

The regrasp has not been sufficiently investigated of body coordinate systems in Lie algebra. The reason for this is the difficulty in understanding relative coordinates in Lie algebra via the body coordinate system. The complexity of the equations has not allowed many researchers to overcome this challenge. The symbolic mathematics toolbox in the Maxima, on the other hand, aided in the systematic formulation of the workspaces in Lie algebra with geodesic and RCT.

The Lie algebra **se(3)** equations presented here have already been developed for robot kinematics from many references. These equations will be used to derive the following workspace types for grasping and regrasping. Body coordinate workspace, spatial coordinate workspace with constraints, body coordinate workspace with constraints, spatial coordinate workspace with constraints are the workspace types. The RCT and geodesic solutions exploit these four fundamental workspace equations derived using Lie algebra.

**Key words:** body coordinate workspace, spatial coordinate workspace, regrasp planning, mechanism, differential geometry

## 1. Introduction

Differential geometry is a strong and highly effective mathematical subject for robot gripper design when grasping within the predetermined trajectories of path planning. This study in grasping focuses on differential geometry analysis



H. Sahin (e-mail: haydar.sahin@gedik.edu.tr) is with İstanbul Gedik University, Engineering Faculty, Mechatronics Engineering Department, İstanbul, Türkiye.

Received 21.09.2022. Revised 04.01.2023.

utilizing the Lie algebra, geodesic, and Riemann Curvature Tensors (RCT). Continuum robots are investigated for grasp purpose [1]. Prior efforts on Lie algebra concentrated on spatial coordinate workspace analysis with constraints [2]. I will look at how the 2R robot's regrasp mechanism affects the relative motions between joints via Lie algebra. The realization of the relative joint motions is made possible by the body coordinate formulation based on Lie algebra se(3).

The relative motion will cause the object to move so that it can be regrasped in a new pose. The relative workspaces of the Lie algebra will also be used to build the trajectories. The analytical outcomes of the geodesic and RCT are exploited to produce these trajectories. The body coordinate workspaces can be used to specify the objects maneuvered and to generate new poses. Additionally, utilizing the body coordinate workspace equations and the geodesic and RCT information, these created trajectories of the regrasp move the object's new pose.

The approach of the body coordinate with the geodesic and RCT is what makes this article unique for 2RR robot mechanisms. The body coordinate and spatial coordinate workspaces can be deduced using Lie algebra se(3). First, these two coordinates are compared in terms of the grasping kinematics of the 2R robot modular gripper mechanisms. The Lie algebra body coordinate workspace focuses on in-hand relative joint motions, whereas the spatial coordinate workspace focuses on grasping in a fixed coordinate system at the base.

The main novelty herein is the comprehensive utilization of the derived body coordinate workspace equations with the geodesic and RCT analyses for trajectory generations of the multi-finger grippers of the 2R mechanism for grasping and regrasping. Furthermore, the toolbox development in this paper is completed for this purpose using Maxima, which is rare in the literature. The grasping and regrasping kinematics have not been thoroughly studied to generate the relative coordinate trajectories using the geodesic equations with an RCT.

The significance of this research is unavoidable, especially in grasping and regrasping objects with varied shapes. In this article, the types of workspaces are clarified and classified for grasping and regrasping kinematics. The regrasp has not been sufficiently investigated in body coordinate systems in Lie algebra. The reason for this is the difficulty in understanding relative coordinates in Lie algebra via the body coordinate system. The complexity of the equations has not allowed many researchers to overcome this challenge.

Maxima's symbolic mathematics toolbox aided in the systematic formulation of the workspaces in Lie algebra with geodesic and RCT. Therefore, explaining body coordinates with the example configurations of the relative motions for regrasping is another crucial goal of this study. Finally, these workspace types will be used to generate trajectories using novel methods of geodesic and RCT. These trajectories are called regrasp or grasp trajectories via RCT and geodesic.

## 2. Fundamentals of the grasping and regrasping kinematics using Lie algebra se(3)

The grasping and regrasping define the workspaces based on the kinematics functionality of the robot grippers. The object shape contains the required mechanism design of the gripper for grasping. The configuration of the mechanisms, along with the dimensions of the limb components, determines the grasping and regrasping kinematics. These configuration types contain the kinematics of the spatial coordinate workspace, body coordinate workspace, constraint-based spatial coordinate workspace, and constraint-based body coordinate workspace. While the body's coordinate workspace establishes the regrasping kinematics, the spatial coordinate workspaces defines the grasping kinematics. The grasp uses fixed (spatial) coordinates at the base and defines the remaining limb components according to this base. These limb components are links, joints, and twists. Meanwhile, regrasping uses determined body coordinates at the limb where the remaining limb component position is defined relative to this determined body coordinate.

Additionally, the constraint-based workspaces requested the ability to grasp or regrasp the convenient object shapes with the constraints. Previously, the angle between C-ISAs (Controllable Instantaneous Screw Axis) was used to determine constraint-based workspaces, as completed in another article [2]. Also, an algorithm-based workspace is composed of multiple robots using Lie algebra **se(3)** [3]. The Lie algebra equations presented here have already been developed for robot kinematics, as shown in Tables 1 and 2 from numerous references [2–6]. These equations of the adjoints and twists are utilized to derive the following workspace types for grasping and regrasping.

Body coordinate workspace, spatial coordinate workspace with constraints, body coordinate workspace with constraints, spatial coordinate workspace with constraints are the workspace types. The RCT and geodesic solutions exploit these four fundamental workspace equations derived using Lie algebra.

These known equations [2–6] are used to program and solve workspace equations, RCT, and geodesic equations in Maxima.

The following Equations of (1) and (2) [2–6] of Lie algebra are used to derive the workspaces.

$$\xi_i' = Ad^{-1}_{\left(e^{\hat{\xi}_i\theta_i}\ldots e^{\hat{\xi}_n\theta_n} g_{0\_2}(0)\right)}\,\xi_i\,, \tag{1}$$

$$\xi_s = Ad_{g_n}\,\xi_b = \begin{pmatrix} -\omega_n \times q_n \\ \omega_n \end{pmatrix}. \tag{2}$$

One example was completed with the results and drawings of all conditions for tw(3) and tw(1), as shown in Table 3. The tables for various adjoint conditions are

Table 1: Notations of grasp and regrasp kinematics for transformation matrix and adjoints

| Twist ($n$) | 0 | 1 | 2 | 3 | 4 |
|---|---|---|---|---|---|
| Indices in between two spatial points for the kinematics | *Base:* 0_0 ***Link 0*** (0_0:$l0$) | *Between base and* ***revolute joint 1*** (0_1$j$:$j1$) | *Between revolute joint 1 and COG of rigid body* ***Link 1*** (1$j$_1:$l1$) | *Between revolute joint 1 and* ***revolute joint 2*** (1$j$_2$j$:$j2$) | *Between revolute joint 2 and COG of rigid body* ***Link 2*** (2$j$_2:$l2$) |
| Twists as C-ISA (wn) (se(3)) | *No rotation* $\xi_{0\_0} = \begin{bmatrix}0\\0\\0\\0\\0\\0\end{bmatrix}$ | *Rotation with screw theory* $\xi^B_{0\_1j} = \begin{bmatrix}0\\0\\0\\\cos(\alpha_1)\cos(\alpha_2)\\-\cos(\alpha_2)\sin(\alpha_1)\\\sin(\alpha_2)\end{bmatrix}$ $\xi^S_{0\_1j} = \begin{bmatrix}0\\0\\0\\\cos(\alpha_1)\cos(\alpha_2)\\-\cos(\alpha_2)\sin(\alpha_1)\\\sin(\alpha_2)\end{bmatrix}$ | *No rotation* $\xi_{1j\_1} = \begin{bmatrix}0\\0\\0\\0\\0\\0\end{bmatrix}$ | *Rotation with screw theory* $\xi^B_{1j\_2j} = \begin{bmatrix}l_1\sin(\alpha_4)\\0\\-l_1\cos(\alpha_3)\cos(\alpha_4)\\\cos(\alpha_3)\cos(\alpha_4)\\-\cos(\alpha_3)\sin(\alpha_4)\\\sin(\alpha_4)\end{bmatrix}$ $\xi^S_{1j\_2j} = \begin{bmatrix}0\\0\\0\\\cos(\alpha_3)\cos(\alpha_4)\\-\cos(\alpha_3)\sin(\alpha_4)\\\sin(\alpha_4)\end{bmatrix}$ | *No rotation* $\xi_{2j\_2} = \begin{bmatrix}0\\0\\0\\0\\0\\0\end{bmatrix}$ |
| Transformation matrix | $g_{0\_1j} = \begin{matrix}1&0&0&0\\0&1&0&0\\0&0&1&0\\0&0&0&1\end{matrix}$ | $g_{0\_1j} = \begin{matrix}1&0&0&0\\0&1&0&0\\0&0&1&0\\0&0&0&1\end{matrix}$ | $g_{1j\_1} = \begin{matrix}1&0&0&0\\0&1&0&r_1\\0&0&1&0\\0&0&0&1\end{matrix}$ | $g_{1j\_2j} = \begin{matrix}1&0&0&0\\0&1&0&l_1\\0&0&1&0\\0&0&0&1\end{matrix}$ | $g_{2j\_2} = \begin{matrix}1&0&0&0\\0&1&0&r_2\\0&0&1&0\\0&0&0&1\end{matrix}$ |
| Adjoints | | $Ad^{-1}_{(g_{0\_1j})}$ | $Ad^{-1}_{(g_{1j\_1})}$ | $Ad^{-1}_{(g_{1j\_2j})}$ | $Ad^{-1}_{(g_{2j\_2})}$ |

defined in the following sections multiplied by twist 1 and twist 3. The Maxima program includes the following equations, as shown in Table 3.

Twists 1 and 3 of the grasping kinematics correspond to the screw axes of joint one and joint 2. The twists' characteristics are described by spatially connected points, which can be a base or a type of joint on two sides. Twist 1 is shown as being between the base and revolutes joint 1, abbreviated as (0_1$j$) for the twists and adjoints in Table 1.

Table 1 shows twist three as being located between revolute joints 1 and 2, denoted as (1$j$_2$j$). This subscript abbreviation is similarly used for both the

Table 2: Notations of grasp and regrasp kinematics in Lie algebra method for ISA of the 2R limb

| $n$ | 0_0 | 0_1$j$ | 1$j$_1 | 1$j$_2$j$ | 2$j$_2 |
|---|---|---|---|---|---|
| Indices in between two spatial points for the kinematics | Base | Between base and revolute joint 1 | Between revolute joint 1 and COG of rigid body link 1 | Between revolute joint 1 and revolute joint 2 | Between revolute joint 2 and COG of rigid body link 2 |
| Joint and COG positions (q) | $q_0 = q_{0\_0}$ | $q_1 = q_{0\_1j}$ | $q_2 = q_{1j\_1}$ | $q_3 = q_{1j\_2j}$ | $q_4 = q_{2j\_2}$ |
| $q$ | $\begin{pmatrix}0\\0\\0\end{pmatrix}$ | $\begin{pmatrix}0\\0\\0\end{pmatrix}$ | $\begin{pmatrix}0\\r_1\\0\end{pmatrix}$ | $\begin{pmatrix}0\\l_1\\0\end{pmatrix}$ | $\begin{pmatrix}0\\r_2\\0\end{pmatrix}$ |
| C-ISA | $\omega_{0\_0} = \begin{bmatrix}0\\0\\0\end{bmatrix}$ $\theta_{0\_0} = 0$ | $\omega_{0\_1j} = \begin{bmatrix}0\\0\\1\end{bmatrix}$ $\theta_{0\_1j} = \theta_1$ | $\omega_{1j\_1} = \begin{bmatrix}0\\0\\0\end{bmatrix}$ $\theta_{1j\_1} = 0$ | $\omega_{1j\_2j} = \begin{bmatrix}\cos\alpha_1\cos\alpha_2\\-\cos\alpha_2\sin\alpha_1\\\sin\alpha_2\end{bmatrix}$ $\theta_{1j\_2j} = \theta_2$ | $\omega_{2j\_2} = \begin{bmatrix}0\\0\\0\end{bmatrix}$ $\theta_{2j\_2} = 0$ |

Table 3: The workspace equations

| Equation number | Expression of the equation | Maxima script | Comments |
|---|---|---|---|
| 1 | $Ad^{-1}_{(g_{1j\_2})}\,\xi^B_{1j\_2j}$ | Adgabt[3, 3]tw[3] | |
| 2 | $Ad^{-1}_{(g_{1j\_2})}\,\xi^B_{0\_1j}$ | Adgabt[3, 3]tw[1] | |
| 3 | $Ad^{-1}_{(g_{1j\_2j})}\,\xi^B_{1j\_2j}$ | Adgabt[3, 2]tw[3] | |
| 4 | $Ad^{-1}_{(g_{1j\_2j})}\,\xi^B_{0\_1j}$ | Adgabt[3, 2]tw[1] | |
| 5 | $Ad^{-1}_{(g_{1j\_1})}\,\xi^B_{0\_1j}$ | Adgabt[2, 2]tw[1] | $\xi^B_{0\_1j}$: Joint twist in body coordinate |
| 6 | $Ad_{(g_{1j\_1})}\,\xi^S_{0\_1j}$ | Adgab[2, 2]tws[1] | $\xi^S_{0\_1j}$: Joint twist in spatial coordinate |
| 7 | $Ad_{(g_{1j\_2j})}\,\xi^S_{0\_1j}$ | Adgab[3, 2]tws[1] | $\xi^S_{1j\_2j}$: Joint twist in spatial coordinate |

twists and adjoints. The connection sequence of the links and joints is link 0, joint 1, link 1, joint 2, and link 2, as seen in Table 1.

Link 1 is related to twist 2, where the transformation matrix is defined with the rigid body's center of gravity (COG) length as $r_1$. The spatial points joint 1 to joint 2 are related to twist 3, where the transformation matrix is characterized by the rigid body length as $l_1$. Link 2 is related to twist 4, where the transformation matrix is defined by the rigid body's COG length as $r_2$.

The abbreviations for the subscripts, for the expression of the equations in Table 3, indicate the base and joint numbers. The base is abbreviated as 0, while joints 1 and 2 are abbreviated as $1j$ and $2j$, respectively. Where (1) and (2) represent the link numbers in the subscripts of the adjoints and twists for Table 3.

All the equations derived from Lie algebra and Maxima in Tables 4–7 have been published in the literature [2–6]. While Adgab[3,3] is concerned with the 2R robot mechanisms, Adgab[2,2] is concerned with the 1R robot mechanisms. Also, Adgab[3,3] arranges the kinematics beginning at the endpoint, while Adgab[3,2] arranges the kinematics starting at the second joint of twist3.

### 2.1. Spatial coordinate workspaces using Lie algebra se(3) for grasping kinematics of the spatial twist 1 ($\xi^S_{0\_1j}$)

Throughout the article, the special cases of $\alpha_{1,2,3,4}$ as being $\pi/2$ are used to verify the derived equations using Lie algebra with the Euclidean or plane geometry. Additionally, this special case will simplify the derived equations via the Lie algebra of differential geometry. Along with understanding relative body coordinates in a simplified equation, it would be pedagogically advantageous to explain coordinate functionality using Euclidean geometry and trigonometry.

The only coordinate used is at point B for the fixed spatial coordinate system. The coordinates of points E and F are only used for the body coordinate workspace determination in Figure 1. The spatial workspace of $Ad_{(g_{1j\_2j})}\,\xi^S_{0\_1j}$ is defined as the position of point A *relative to the fixed coordinate* at point B in Figure 1. The spatial second joint twist concerning the base is defined relative to the end of the $l_1$ of point D, as in Figure 1.

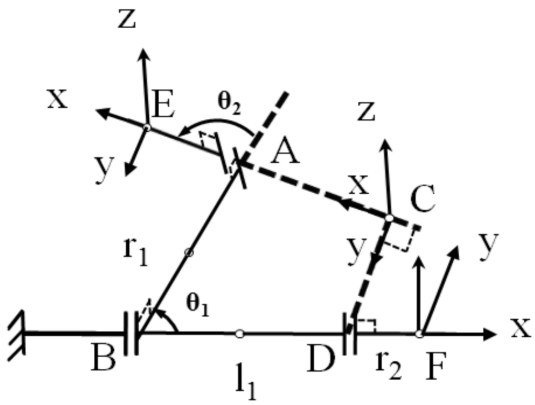


Figure 1: The generated grasping and regrasping configuration of the $\alpha_{1,2,3,4} = \pi/2$ for varied $\theta_1$ and $\theta_2$ using twist 3 with adjoint of $Ad_{(g_{1j\_2})}$ or $Ad^{-1}_{(g_{1j\_2})}$

Since the joint is directly connected to the fixed base, the body twists coordinate result on point B ($\xi^B_{0\_1j}$) is equal to the spatial twist coordinate result on

point B ($\xi^S_{0\_1j}$) of Figure 1. The $Ad_{(g_{1j\_2j})}\,\xi^S_{0\_1j}$ workspace represents the spatial second joint twist in relation to the base. The workspace of the joint 2 location is defined with respect to the base of point B, as shown in Figure 1. The twist equations are derived using the screw axis, which is critical for designing grasping and regrasping kinematics.

The spatial position of the COG of the first rigid body $r_1$ is according to the spatial coordinate on point B of the base for $Ad_{(g_{1j\_1})}\,\xi^S_{0\_1j}$, as seen in Table 4 and Figure 1. The $Ad_{(g_{1j\_1})}$ is related to the 1R robot mechanism. As shown in Table 4, only the $\theta_1$ angles exist as shown in Table 4, since both adjoint and twist are in the range of base and COG of link 1. When $\alpha_{1,2}$ are equal to the $\pi/2$, the workspace result is $[r_1.\cos(\theta_1), r_1.\sin(\theta_1), 0, 0, 0, 1]$, which can be verified geometrically for 1R robot mechanism with one link one joint.

Table 4: The $Ad_{(g_{1j\_2j})}$, $Ad_{(g_{1j\_2})}$ and $Ad_{(g_{1j\_1})}$ adjoints for twist 1 in spatial coordinate

| | |
|---|---|
| $Ad_{(g_{1j\_2})}\,\boldsymbol{\xi}^S_{0\_1j}$: Adgab[3, 3].tws[1], $\alpha_{1,2,3,4} = \pi/2$ $\begin{pmatrix} r_2\cos(\theta_1+\theta_2)+l_1\cos(\theta_1) \\ r_2\sin(\theta_1+\theta_2)+l_1\sin(\theta_1) \\ 0 \\ 0 \\ 0 \\ 1 \end{pmatrix}$ see Figure 1 | $Ad_{(g_{1j\_2j})}\,\boldsymbol{\xi}^S_{0\_1j}$: Adgab[3, 2]tws[1], $\alpha_{1,2,3,4} = \pi/2$ $\begin{pmatrix} l_1\cos(\theta_1) \\ l_1\sin(\theta_1) \\ 0 \\ 0 \\ 0 \\ 1 \end{pmatrix}$ see Figures 1 and 4 |
| $Ad_{(g_{1j\_1})}\,\boldsymbol{\xi}^S_{0\_1j}$: Adgab[2, 2]tws[1] $\alpha_{1,2}$ are equal to the $\pi/2$, 1-R robot mechanism $[r_1\cos(\theta_1),\ r_1\sin(\theta_1),\ 0,\ 0,\ 0,\ 1]$ | |

The relative position of the E is described herein as in Table 4 for $Ad_{(g_{1j\_2})}\,\xi^S_{0\_1j}$. Thus, the distance determination of point E is *relative to the fixed coordinates* of point B, as seen in Figure 1. While tw1 or tw3 can be used to form the body coordinate workspace, Table 1 demonstrates that tw1 and tw3 are the same for the spatial coordinate.

### 2.2. Spatial coordinate workspaces using Lie algebra se(3) for grasping kinematics of the spatial twist 3 ($\xi^S_{1j\_2j}$)

The matrix of body adjoint of $Ad_{(g_{1j\_2})}$, which is between the first joint and the COG of the second link, transforms the second spatial joint twist ($\xi^S_{1j\_2j}$). This mathematical operation defines the spatial position of the end effector at point E with respect to *the fixed coordinate system* at the base, as shown in Figure 1. The spatial joint twist and body adjoints determine spatial configuration manipulation where the workspace of the end-effector is determined relative to

the base. The $\xi^S_{1j\_2j}$'s spatial twist is between revolute joints 1 and 2, where the $l_1$ length is active for the transformation matrix, as shown in Table 1.

The body twists coordinate result on point ($\xi^B_{1j\_2j}$) is not equal to the spatial twist coordinate result on point A ($\xi^S_{1j\_2j}$) of Figure 1, since the joint 2 is not directly connected to the base, as shown in Table 1. The joint 2 of Twist 3 is connected to link1 on one side and link 2 on the other, as in Table 1's twist equation. The second body joint twist transforms with the matrix of body adjoint between the first joint and the COG of the second link, the end effector, as in Table 1.

The different configuration manifolds for 2-RR grasping and regrasping are created by changing the shape of the variable angles of $\theta_1$ and $\theta_2$. The Maxima equations of workspaces are for spatial coordinates and body coordinates as Adgab[3,3]tws[1] and Adgabt[3,3]tw[1], respectively.

Since the spatial twist of tws3 and tws1 are equal, as seen in Table 1, the result in Table 5 for $Ad_{(g_{1j\_2})}\,\xi^S_{1j\_2j}$ is the same with Table 4 for $Ad_{(g_{1j\_2})}\,\xi^S_{0\_1j}$. The $Ad_{(g_{1j\_2j})}\,\xi^S_{1j\_2j}$ workspace is generated with the spatial second joint twist with respect to *the fixed coordinate system at base*. The equation in Table 4 can be derived from Figure 1 for point A. The link is defined as the distance between the rigid body's joint and its center of gravity.

Table 5: The $Ad_{(g_{1j\_2j})}$, and $Ad_{(g_{1j\_2})}$ adjoints are for tw3 in spatial coordinate workspaces

| | |
|---|---|
| $Ad_{(g_{1j\_2})}\,\xi^S_{1j\_2j}$: Adgab[3,3]tws[3]<br>$\alpha_{1,2,3,4} = \pi/2$<br>$\begin{pmatrix} r_2\cos(\theta_1+\theta_2)+l_1\cos(\theta_1) \\ r_2\sin(\theta_1+\theta_2)+l_1\sin(\theta_1) \\ 0 \\ 0 \\ 0 \\ 1 \end{pmatrix}$ see Figure 1 | $Ad_{(g_{1j\_2j})}\,\xi^S_{1j\_2j}$: Adgab[3,2]tws[3]<br>$\alpha_{1,2,3,4} = \pi/2$<br>$\begin{pmatrix} l_1\cos(\theta_1) \\ l_1\sin(\theta_1) \\ 0 \\ 0 \\ 0 \\ 1 \end{pmatrix}$ see Figures 1 and 4 |

### 2.3. Body coordinate workspaces using Lie algebra se(3) for regrasping kinematics of the twist 1 ($\xi^B_{0\_1j}$)

The spatial position for the twist of the $\xi^S_{0\_1j}$, relative to the spatial coordinate on point D of the base, is for the end point of the $r_1$ or $l_1$ relative to point D in Figure 2. Since the connected base of the D is fixed, the relative body coordinate of the endpoint $\xi^B_{0\_1j}$ equals the spatial coordinate $\xi^S_{0\_1j}$ endpoint, as shown in Figure 2. Table 6 displays all workspace equations established using twist1 of $\xi^B_{0\_1j}$ for the body coordinate system. Also, Table 1 reveals the twist equations.

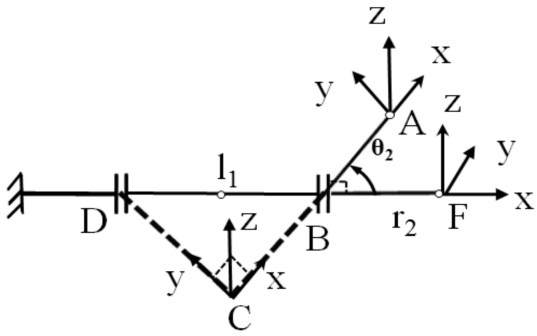


Figure 2: The generated regrasping configuration of the $\alpha_{1,2,3,4} = \pi/2$ for varied $\theta_2$ using twist 1 with adjoint of $Ad^{-1}_{(g_{1j\_2})}$ where the equation in Maxima is Adgabt[3,3]tw[1]

The coordinate system is depicted at the end effector point of A as shown in Table 1, the twist $\xi^B_{0\_1j}$ is located between the base and revolute joint 1. The positional location of the end effector at point A in Figure 2 is defined relative to twist 1 and dependent on the coordinates of D. The generalized equation of the body coordinate workspace $Ad^{-1}_{(g_{1j\_2})}\,\xi^B_{0\_1j}$ is defined as Adgabt[3,3]tw[1], as shown in Table 3 of Maxima. The end effector positional workspace relative to joint 1 is for the configuration of Figure 2 with substituted values of the $\alpha_{1,2,3,4}$ as $\pi/2$. Since we only have the $\theta_2$ rotation, as shown in Figure 2, the configurational workspace does not contain $\theta_1$, as in the Table 6.

Table 6: The $Ad^{-1}_{(g_{1j\_2j})}$, $Ad^{-1}_{(g_{1j\_2})}$ and $Ad^{-1}_{(g_{1j\_1})}\,\xi^B_{0\_1j}$ workspaces are for tw1 in body coordinate

| | |
|---|---|
| $Ad^{-1}_{(g_{1j\_2})}\,\xi^B_{0\_1j}$: Adgabt[3,3]tw[1], $\alpha_{1,2,3,4} = \pi/2$ $\begin{pmatrix} -r_2 - \cos(\theta_2) l_1 \\ \sin(\theta_2) l_1 \\ 0 \\ 0 \\ 0 \\ 1 \end{pmatrix}$ see Figure 2 | $Ad^{-1}_{(g_{1j\_2j})}\,\xi^B_{0\_1j}$: Adgabt[3,2]tws[1], $\alpha_{1,2,3,4} = \pi/2$ $\begin{pmatrix} -l_1 \cos(\theta_2) \\ l_1 \sin(\theta_2) \\ 0 \\ 0 \\ 0 \\ 1 \end{pmatrix}$ see Figure 3 |
| $Ad^{-1}_{(g_{1j\_1})}\,\xi^B_{0\_1j}$: Adgabt[2,2]tw[1], When $\theta_1 = \pi$, as follows $\alpha_{1,2}$ are equal to the $\pi/2$, 1-R robot mechanism $[-r_1, 0, 0, 0, 0, 1]$ | |

Here the body twist coordinate result on point D ($\xi^B_{0\_1j}$) is equal to the spatial twist coordinate result on point D ($\xi^S_{0\_1j}$) of Figure 2 since one side of the joint

is directly connected to the base. The joint is connected to the base on one side and link 1 on the other side, as shown in the twist equation of Table 1. The result is relative to the base (D) according to the body coordinate (xyz) on point A of Figure 2. Only $\theta_2$ is effective since the relative motion is only available between points B and A. The description of point D is according to the coordinate system of point A in Figure 2.

The $Ad^{-1}_{(g_{1j\_2})}\,\xi^{B}_{0\_1j}$ is programmed in the Maxima as Adgabt[3,3]tw[1], which contains the substituted values of the $\pi/2$ for $\alpha_{1,2,3,4}$. The aim herein is to generate Euclidean geometrical analyses to explain and verify the body coordinate equation results via Lie algebra. Also, the Lie algebra results are simplified with this substitution for the $\alpha_{1,2,3,4}$. The position of the end-effector is described relative to joint 1. The starting and final positions of the endpoint of the $r_2$ determine the body coordinate at point A.

The body coordinate workspace $Ad^{-1}_{(g_{1j\_1})}\,\xi^{B}_{0\_1j}$ is defined in terms of $r_1$ for specified values of the $\alpha_{1,2}$ and $\theta_1$, as seen in Table 6. This body coordinate workspace obtains the 1R robot mechanism with one link and one joint that defines the position of the end of the $r_1$ in Figure 3. The position of point D with respect to the end of the $r_1$ is calculated using this workspace equation and the coordinates on the endpoint of the $r_1$. The position of the COG of the first link as $r_1$ is defined relative to point D, which is according to the coordinates of the endpoint of $r_1$, as shown in Figure 2.

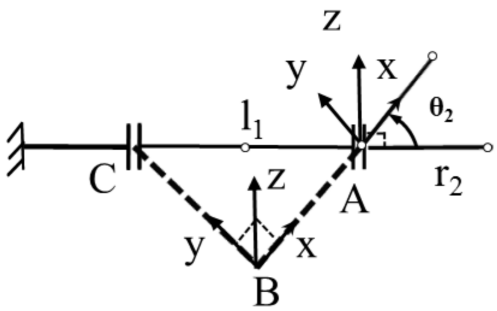


Figure 3: The generated regrasping configuration of the $\alpha_{1,2,3,4} = \pi/2$ for varied $\theta_2$ using twist 1 with adjoint of $Ad^{-1}_{(g_{1j\_2j})}$ which is $Ad^{-1}_{(g_{1j\_2j})}\,\xi^{B}_{0\_1j}$ of Adgabt[3,2].tw[1] in Maxima

The body coordinate workspace equation $Ad^{-1}_{(g_{1j\_2j})}\,\xi^{B}_{0\_1j}$ is defined with the inverse of the adjoint in between the joint 1 and 2. The joint 2 location on point A of Figure 3 is defined relative to the initial location of twist 3 (joint 2). Similarly, the body joint twists of the second joint are defined with respect to the second link. This equation contains $\theta_2$ and $l_1$, as seen in Table 6. Only $\theta_2$ is effective for configuration in Figure 3 of the derived Lie algebra equations.

Joint (2) position is defined in the adjoint equation $Ad^{-1}_{(g_{1j\_2j})}\,\xi^{B}_{0\_1j}$ with 2j as a subscript, the equation is relative to *the initial location* of $r_2$'s endpoint. However, the spatial coordinates are considered fixed coordinates on the base. The coordinate system start point will be established on point A of the joint to describe location C, as shown in Figure 3. This description of point C is according to the coordinate system of point A in Figure 3.

As shown in Figure 3, this mathematical operation defines the position of the second joint, point A relative to point C. Body joint twist and body adjoints determine configuration manipulation. Two effective parameters for the definition of point A of the second joint are $l_1$ and $\theta_2$ according to the relative coordinates of point A of the relative coordinates, as shown in Figure 3. The joint 2 location is defined relative to the initial location of twist 1 (joint 1). The configuration manipulation is determined by the body joint twist and the inverse of the body adjoints.

### 2.4. Body coordinate workspaces using Lie algebra se(3) for regrasping kinematics of the twist 3 ($\xi^{B}_{1j\_2j}$)

Second joint twist multiplies the inverse of the adjoint of the second body joint. The configuration manipulation is determined via the body joint twist and body adjoints. The second body joint twist transforms with the matrix of body adjoint between the first and second joint, as seen in Table 1. This mathematical operation defines the position of the second joint at point A with respect to point D of twist 3, as shown in Figure 4. Body adjoints mean the inverse of the adjoint.

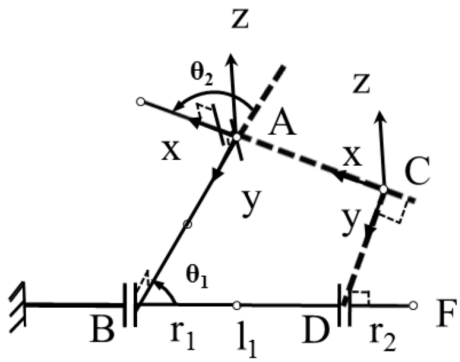


Figure 4: The generated regrasping configuration of the $\alpha_{1,2,3,4} = \pi/2$ for varied $\theta_1$ and $\theta_2$ using twist 3 with adjoint of $Ad^{-1}_{(g_{1j\_2j})}$ which is $Ad^{-1}_{(g_{1j\_2j})}\,\boldsymbol{\xi}_{1j\_2j}$ of Adgabt[3,2].tw[3] in Maxima

The joint 2 location A for $Ad^{-1}_{(g_{1j\_2j})}\,\xi^{B}_{1j\_2j}$ is relative to the initial location of the twist3 (joint 2) $\xi^{B}_{1j\_2j}$ of point D. This description of point D is defined relative to the coordinate system of point A in Figure 4. While the point A coordinate

system in Figure 4 is due to the $Ad^{-1}_{(g_{1j\_2j})}$, the relative position definition of point D is due to the multiplication with the $\xi^{B}_{1j\_2j}$ for the body coordinate workspace. The body coordinate of Lie algebra is necessary for the in-hand motion of the regrasp.

The next section describes the trigonometry of the geometry as well as the verification of the Lie algebraic kinematics equations. This verified equation in body coordinate $Ad^{-1}_{(g_{1j\_2})}\,\xi^{B}_{1j\_2j}$ is to define the workspace owing section 2.5 from Table 7. The equation with the substitution of the $\alpha_{1,2,3,4}$ as $\pi/2$, as seen in Table 4, is derived using Maxima for the body coordinate workspace equation of $Ad^{-1}_{(g_{1j\_2})}\,\xi^{B}_{1j\_2j}$. The $Ad^{-1}_{(g_{1j\_2})}\,\xi^{B}_{1j\_2j}$ defines the link 2 of the end effector position at point E with respect to the initial position of point F, where (2) is a subscript for link2 in the inverse of the adjoint equation. The positioning result is for the (D) relative to the body coordinate $(xyz)$ on point E of Figure 5 and Figure 1. This mathematical operation defines the final position of the end effector, point E, relative to the initial position of the second revolute joint location, point D, as shown in Figure 1.

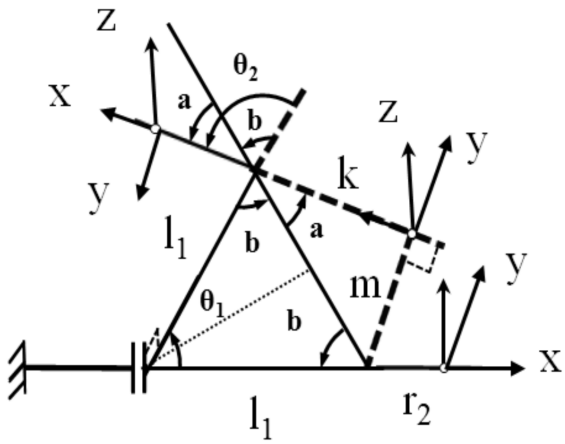


Figure 5: The fundamental equations to derive the Table 1 equations for $\alpha_{1,2,3,4}$ substituted with $\pi/2$ of $Ad^{-1}_{(g_{1j\_2})}\,\xi^{B}_{1j\_2j}$

The difference between multiplying with twist1 or twist3 in body coordinates is the position determination according to the twist1 or twist 3 (joint 2) relative to the coordinate at point E, as seen in Figure 1. The positional definition of point D relative to the coordinate at point E for the inverse of the adjoint $Ad^{-1}_{(g_{1j\_2})}$, multiplied by the twist3, is shown in Figure 1. In contrast, Figure 2 specifies point D relative to the coordinate at point A for the inverse of the adjoint $Ad^{-1}_{(g_{1j\_2})}$ multiplied by the twist1.

One can see this difference in terms of the initial position of point F in Figure 1 and Figure 2. This description of point D is according to the coordinate system of point E in Figure 1. If the inverse of adjoint is multiplied with twist 1, the body coordinate workspace will result according to the twist 1 location of point B in Figure 4. Otherwise, the body coordinate workspace will be established relative to twist 3 of joint 2. The regrasping of the body coordinate workspace via the inverse of the adjoint as of $Ad^{-1}_{(g_{1j\_2j})}$ should use twist3 to determine point D or twist1 to determine point B relative to the coordinate on point A in Figure 4.

Also, the configurational difference between Figure 1 and Figure 2 is one moves the second joint of twist 3 whereas the other does not move the second joint at all. These configurations are determined based on derived equations via Lie algebra se(3) and Maxima. The body twist will be based on how the things in your hands are regrasped in the workspace equation's body coordinate adjoint. We shall multiply by the twist1 if we intend to reorient the object in relation to the twist1 and vice versa for twist3. The derivation process is revealed using geometry in the following Section 2.5.

Table 7: The $Ad^{-1}_{(g_{1j\_2j})}$ and $Ad^{-1}_{(g_{1j\_2})}$ adjoints are for tw3 in body coordinate

| | |
|---|---|
| $Ad^{-1}_{(g_{1j\_2})}\,\xi^{B}_{1j\_2j}$: Adgabt[3,3].tw[3], $\alpha_{1,2,3,4} = \pi/2$ $\begin{pmatrix} l_1\cos(\theta_1+\theta_2) - r_2 - l_1\cos(\theta_2) \\ -l_1(\sin(\theta_1+\theta_2) - \sin(\theta_2)) \\ 0 \\ 0 \\ 0 \\ 1 \end{pmatrix}$ see Figure 1 | $Ad^{-1}_{(g_{1j\_2j})}\,\xi^{B}_{1j\_2j}$: Adgabt[3,2]tw[3] $\alpha_{1,2,3,4} = \pi/2$ $\begin{pmatrix} l_1\cos(\theta_1+\theta_2) - l_1\cos(\theta_2) \\ -l_1(\sin(\theta_1+\theta_2) + \sin(\theta_2)) \\ 0 \\ 0 \\ 0 \\ 1 \end{pmatrix}$ see Figure 4 |

### 2.5. Proof of the body coordinate of the $Ad^{-1}_{(g_{1j\_2})}\,\xi^{B}_{1j\_2j}$ workspace configuration in Lie algebra using trigonometry of the geometry for regrasping kinematics

The special case of the $\alpha_{1,2,3,4}$ with $\pi/2$ is used to arrange proof case in trigonometry. The derived kinematic equations are verified and validated trigonometrically for the manifold of the shape variable angles of the $\alpha_{1,2,3,4}$ substituted with $\pi/2$, as shown in Figure 5. The geometric result in Figure 5 is the same as the derived equation from Lie algebra as below. The derived equations of the (3) and (4) are proved to be the same with the Lie algebra result in Table 7.

$$m = -l_1\left(\sin(\theta_1+\theta_2) - \sin(\theta_2)\right), \tag{3}$$

$$k = l_1\cos(\theta_1+\theta_2) - r_2 - l_1\cos(\theta_2). \tag{4}$$

The following eight equations are manipulated to derive $Ad^{-1}_{(g_{1j\_2})}\,\xi^{B}_{1j\_2j}$ equation on $x$ axis for $k$, and $y$ axis for $m$.

**1.** $\cos(\theta_1/2+\theta_2)=\cos(\theta_1/2)\cos(\theta_2)-\sin(\theta_2)\sin(\theta_1/2)$,
**2.** a +b $=\theta_2$, **3.** 2b+ $\theta_1=180$,
**4.** $\sin(\theta_1/2+\theta_2)=\sin(\theta_1/2)\cos(\theta_2)+\sin(\theta_2)\cos(\theta_1/2)$,
**5.** $\sin(a)=\sin(\theta_2+\theta_1/2)$, **6.** $\cos(a)=\cos(\theta_2+\theta_1/2)$,
**7.** $2l_1\times\sin(\theta_1/2)\sin(a)=m$, **8.** $2l_1\times\sin(\theta_1/2)\cos(a)=k$.

## 3. Results

Only the chosen regrasp workspaces for the 2RR robot gripper will be discussed in this article after using the workspaces for various grasping and regrasping applications. These selected parameters are $\theta_1$ and $\alpha_1$ for the body coordinate that is related to the regrasp. The combinations of the remaining parameters are not included due to the space limitation of the article. Finally, only the body coordinate workspace is covered to show the doability of the generation of the trajectories via RCT and geodesic solutions. The RCT and geodesic solutions are based on four fundamental workspace equations derived using Lie algebra. The parametric derivations of the geodesic with RCT are completed for any combinations of the selected parameters of the ($r_1$, $l_1$, $r_2$, $\alpha_{1,2,3,4}$, $\theta_{1,2}$) using Lie algebra **se(3)**. I will only reveal the result of the combination of the $\theta_1$ and $\alpha_1$ parameters herein.

### 3.1. Body coordinate workspace of the regrasp for the generation of the trajectories via the RCT and geodesic solution results

The body coordinate workspace equation Adgabt[3,3]tw[3], which is defined using the parameters shown in Table 8, is used in this section. As shown in Table 8, the $\theta_1$ and $\alpha_1$ parameters serve to solve the geodesic equations with the initial conditions (IC).

Table 8: The $Ad^{-1}_{(g_{1j\_2j})}$ and $Ad^{-1}_{(g_{1j\_2})}$ adjoints are for tw3 in body coordinate

| $\alpha[1]$ | $\alpha[2]$ | $\alpha[3]$ | $\alpha[4]$ | Adgabt[3,3].tw[3] | $r_1$ | $l_1$ | $\theta_2$ | $r_2$ | $\theta_1$ |
|---|---|---|---|---|---|---|---|---|---|
| $\alpha_1$ | $\pi/6$ | $\pi/2$ | $\pi/2$ | | 0.01 | 0.002 | $\pi/3$ | 0.01 | $\theta_1$ |
| IC | | | | | | | | | IC |
| 0.01 | | | | | | | | | 0.01 |

The RCT components of R1212, R1112, R1121, and R1211 were examined for geodesic solutions. These sectional curvatures enable the construction of

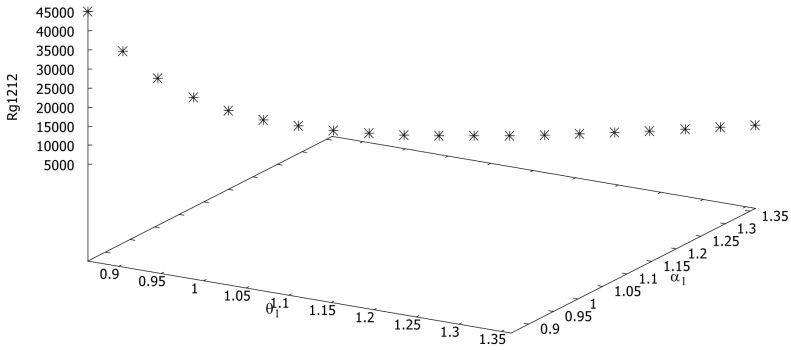


Figure 6: The regional sectional Riemann curvature radius of R1212 for 2RR mechanism is in between −5 and 50000 where the angles are in radians

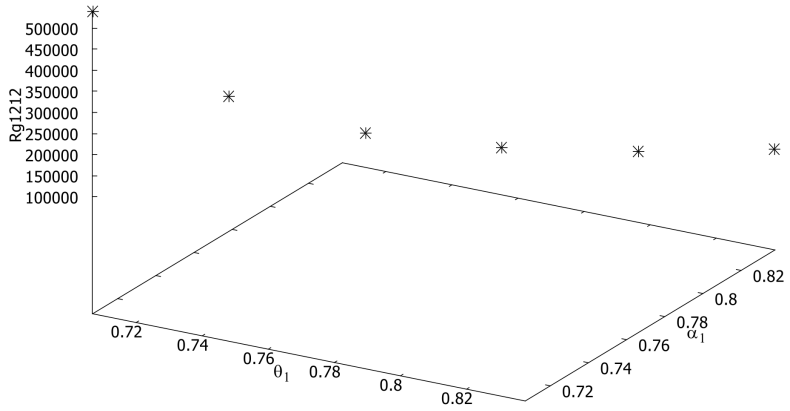


Figure 7: The regional sectional Riemann curvature radius of R1212 for 2RR mechanism is in between 50000 and 1000000 where the angles are in radians

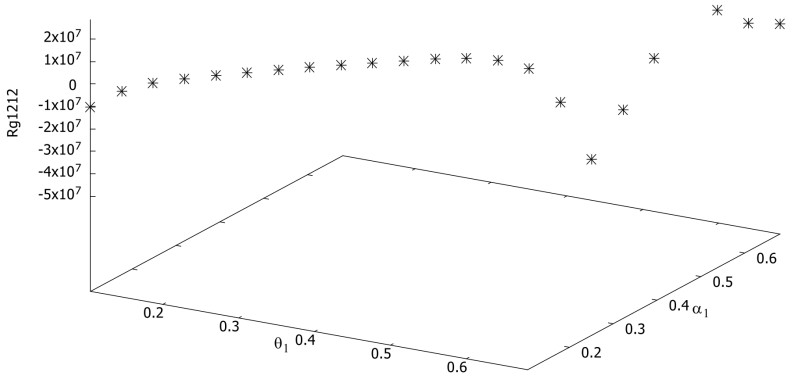


Figure 8: The regional sectional Riemann curvature radius of R1212 for 2RR mechanism is remainings of the curvature values where the angles are in radians

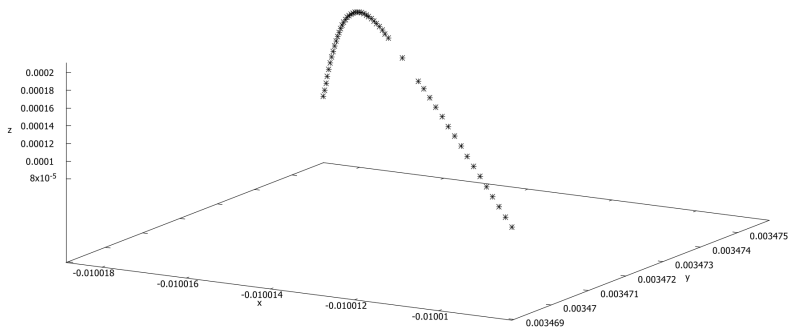


Figure 9: The geodesic trajectory generation of the 2RR robot workspace for regrasping where the unit is in meters. The body coordinate generates path for $\alpha_1$, $\theta_1$ parameters

spatial geometrical trajectories for regrasping. Due to space limitations, only the R1212 result is included in the article.

## 4. Discussions

Precision and power grasp dependent on fingertip relative motions define grasp kinematics. Use of the coordinates determined on the fingertip or joint is inevitable. Finally, the body coordinate workspace of the Lie algebra is investigated for this purpose here with geodesic and Riemann curvature solutions. Additionally, the regrasp is a unique motion where the body coordinate kinematics of the Lie algebra is the pivotal defining in-hand motion of object re-orientations. Therefore, planning is critical for regrasp purpose which requires kinematics well established including the geodesic and RCT. The developed regrasped algorithms are using the fixtures in literature [5–10] without considering in-hand kinematic equations with Lie algebra as completed herein. Thus, the regrasp algorithms and plannings should be redefined using the fundamental and analytical results of the study completed herein.

The trajectories of a geodesic with a RCT are shown in Figures 6–9. The grasp trajectories can be created using the spatial coordinate, since the object will be at the fixed coordinate where it can be grasped by the 2R robot gripper mechanism. The body coordinate can be used to regrasp the object in hand, allowing the joints to be moved around to adjust the reorientation of the object. The constraint angle between the screw axes on joint one and joint two can be used to create modular trajectories. The multimodel planning is used for the grasping and regrasping [5–10].

Grasp plans can be defined based on regrasping possibilities. A grasp pose can be established between the gripper mechanism and the surface manifold of

the object wherein the contact between them occurs. The regrasp configuration is afterward positioned depending on where the object makes contact with the joints, links, and twists as covered herein. Therefore, the geodesic and RCT are based on the generated workspace of the regrasp configurations.

The regrasping kinematics can be defined using relative motions since the object will already be in contact with the varied limbs and joints of the gripper mechanisms. Therefore, the body coordinate system with Lie algebra is utilized to derive the relative workspace equations, which will be relative to the joints. Regrasp trajectories exploit the relative workspace with planning for the reorientation of the objects. The motions are defined using calculated geodesic RCTs between the joints with defined relative workspace trajectories. The manifolds established by the motion of the robot mechanism and the object surface manifolds may intersect on the trajectories that are generated by RCT.

## 5. Conclusion

Grasping various shapes via robotic multi-finger mechanisms is achievable using the kinematics of the varied definable RCT with geodesic for selected parameters of the $(r_1, l_1, r_2, \alpha_{1,2,3,4}, \theta_{1,2})$ using Lie algebra **se(3)**. Applications of the body and spatial twists and adjoints are proved to be convenient for regrasping and grasping purposes using Lie algebra for gripper kinematic design. The RCT is utilized with success using the sectional curvature components of the R1221, R1121, R1212, and R1211 for grasping and regrasping purposes. The novel trajectories are generated using geodesic for regrasping of the various shaped objects.

The regrasping is defined by the body coordinate workspace of the geodesic and RCT. Similarly, the spatial coordinate workspace of the geodesic and RCT results in grasping. Therefore, the grasping and regrasping plans are obtainable based on the novel method developed herein. Trajectories are determined using geodesic and RCT.

The Maxima is programmed with the workspace equations for the spatial coordinate workspace, body coordinate workspace, constraint-based spatial coordinate workspace, and constraint-based body coordinate workspace. The substituted values of the $\pi/2$ for $\alpha_{1,2,3,4}$ are validated and verified for the body coordinate and spatial coordinate workspaces herein. The aim herein is to generate Euclidean geometrical analyses to explain and verify the body coordinate results via Lie algebra. The Lie algebra results are also simplified with this substitution for the $\alpha_{1,2,3,4}$. The rules for grasping and regrasping can be redefined and rephrased as a result of this research article. The research on regrasping up to this point hasn't been as thorough as the research presented here, which combines Lie algebra,

geodesic, and RCT. The wholistic approach for grasping and regrasping herein is unique to lead an applicable planning for the varied shapes using them.

In the future, grasping kinematics should continue to be developed analytically using Lie algebra, geodesics, and RCT. The surface intersections of the object can obtain grasp and regrasp with the 2R and 1R mechanisms developed herein. Multiple robot mechanisms integrate to design the gripper for various grasping purposes using geodesic and RCT.

**Conflict of interest:** This research did not receive any specific grant from funding agencies in the public, commercial, or not-for-profit sectors.

## References

[1] M. Ali and J. Farrokh: Grasp synthesis of continuum robots. *Mechanism and Machine Theory*, **168** (2022), 1–31. DOI: 10.1016/j.mechmachtheory.2021.104575.

[2] S. Haydar: The modular nonoverlapping grasp workspaces and dynamics for the grippers using the micro and macro C-manifold design. *Journal of Scientific & Industrial Research*. **80**(9), (2021), 766–776. DOI: 10.56042/jsir.v80i09.47040.

[3] S. Haydar: Algorithmic workspace programming of the collaborative multi-robots. *Osmaniye Korkut Ata Üniversitesi Fen Bilimleri Enstitüsü Dergisi*, **5**(1), (2022), 325–341. DOI: 10.47495/okufbed.1030575.

[4] A. Müller: Screw and Lie group theory in multibody dynamics recursive algorithms and equations of motion of tree-topology systems. *Multibody System Dynamics*, **42** (2018), 219–248. DOI: 10.1007/s11044-017-9583-6.

[5] A.S. Morgan, K. Hang, B. Wen, K. Bekris, and A.M. Dollar: Complex in-hand manipulation via compliance-enabled finger gaiting and multimodal planning. *IEEE Robotics and Automation Letters*, **7**(2), (2022), 4821–4828. DOI: 10.1109/LRA.2022.3145961.

[6] Z. Xian, P. Lertkultanon and Q.-C. Pham: Closed-chain manipulation of large objects by multi-arm robotic systems. *IEEE Robotics and Automation Letters*, **2**(4), (2017), 1832–1839. DOI: 10.1109/LRA.2017.2708134.

[7] J. Ma, W. Wan, K. Harada, Q. Zhu, and H. Liu: Regrasp planning using table object poses supported by complex structures. *IEEE Transactions on Cognitive and Developmental Systems*, **11**(2), (2019), 257–269. DOI: 10.1109/TCDS.2018.2868425.

[8] A. Sintov, O. Tslil, and A. Shapiro: Robotic swing-up regrasping manipulation based on the impulse–momentum approach and cLQR control. *IEEE Transactions on Robotics*, **32**(5), (2016), 1079–1090. DOI: 10.1109/TRO.2016.2593053.

[9] Y. Zheng, F.F. Veiga, J. Peters, and V.J. Santos: Autonomous learning of page flipping movements via tactile feedback. *IEEE Transactions on Robotics*, Early Access, 1–16, (2022). DOI: 10.1109/TRO.2022.3168731.

[10] A. Palleschi, G.J. Pollayil, M.J. Pollayil, M. Garabini, and L. Pallottino: High-level planning for object manipulation with multi heterogeneous robots in shared environments. *IEEE Robotics and Automation Letters*, **7**(2), (2022), 3138–3145. DOI: 10.1109/LRA.2022.3145987.